Available online at www.sciencedirect.com
ScienceDirect
Journal of Power Sources 178 (2008) 34–43
JOURNAL OF POWER SOURCES
www.elsevier.com/locate/jpowsour

Characterization of direct formic acid fuel cells by Impedance Studies: In comparison of direct methanol fuel cells

Sunghyun Uhm [a,b], Sung Taik Chung [a], Jaeyoung Lee [b,*]

[a] *Department of Chemical Engineering, Inha University, Inchon 402-751, Republic of Korea*
[b] *Electrochemical Reaction and Technology Laboratory (ERTL), Department of Environmental Science and Engineering, Gwangju Institute of Science and Technology, Gwangju 500-712, Republic of Korea*

Received 6 November 2007; received in revised form 2 December 2007; accepted 3 December 2007
Available online 15 December 2007

Abstract

We characterized direct liquid fuel cells by electrochemical impedance spectroscopy (EIS) combined with reversible hydrogen electrode (RHE) under fuel cell operating conditions. EIS has been successfully implemented as an in-situ diagnostic tool using an impedance setup with RHE, capable of singling out individual contributions to the overall polarization of fuel cells and separating the anode and cathode contributions. While a direct methanol fuel cell (DMFC) anode was subject to substantial poisoning by reaction intermediates due to better accessibility of methanol to catalyst surface regardless of anode diffusion media, a direct formic acid fuel cell (DFAFC) anode suffered from significant mass transfer limitation depending on the anode diffusion media property and formic acid concentration. The high frequency resistance of a DFAFC cathode increased linearly with an increase of formic acid concentration by membrane dehydration effect. Interestingly, on both the DMFC and DFAFC cathodes, decrease in the mixed charge transfer resistance with an increase of fuel crossover was observed together with a drop in the cathode potential.

Keywords: DLFC; EIS; RHE; Anode diffusion media; Mixed charge transfer resistance

1. Introduction

The practical use of direct liquid fuel cells (DLFCs), given their relatively simple system design and cell operation [1–12], is expected as a promising candidate for portable energy sources. However, many obstacles such as the low electrocatalytic activity of liquid fuel, low fuel efficiency due to fuel crossover, and questionable long-term durability still prevent their widespread commercial application.

In order to extend the practical application of DLFCs and facilitate their penetration into the market, it is also desirable to increase the number of liquid fuels that can be employed in these devices. Until now, the most promising one was methanol and formic acid owing to its high energy density. However, despite of significant progress in the fundamental DLFC research, there has a growing need for new and powerful diagnostic tools, capable of providing more useful information on the performance, particularly the identification of performance issue of their individual components such as anode, polymer electrolyte, and cathode.

So far, diagnostic tools of DLFCs are practically limited to the use of various dc electrochemical techniques. These techniques can provide only the sum of various cell polarizations, which is difficult to break down into individual polarization contributions. Contrary to dc techniques, electrochemical impedance spectroscopy (EIS) has long been used to probe the interfacial process and species in electrochemical systems. Specifically, it has proved to be very useful in distinguishing processes with different time constants, and with this method it might be possible to separate different elementary steps of the reaction [13,14]. Although several studies have used EIS to investigate the methanol oxidation in a direct methanol fuel cell (DMFC) [15–19], there have been few reports focusing on formic acid oxidation in a direct formic acid fuel cell (DFAFC) to our knowledge [5]. EIS analysis of electrochemical process in real electrode environment is very important not only to have a clearer understanding of the reaction, but also to avoid artifact arising from other components or environments.

* Corresponding author.
E-mail address: jaeyoung@gist.ac.kr (J. Lee).

0378-7753/$ – see front matter © 2008 Elsevier B.V. All rights reserved.
doi:10.1016/j.jpowsour.2007.12.016

Furthermore, it is necessary to measure the individual electrode potentials and impedance spectra in order to understand the distribution of the voltage losses and polarization contributions of individual electrode. Until now, several attempts have been made to investigate these electrode effects separately by introducing a reference electrode. However, due to the constraints of the cell construction and the requirement of physical contact with the electrolyte, it is rather difficult to place a reference electrode in the cell. Instead, dynamic hydrogen counter/pseudo-reference electrode is commonly used as the reference electrode [15,19–21]. For example, cathode impedance in DMFC can be obtained by subtracting anode impedance from full-cell impedance. Dynamic hydrogen electrode (DHE) is another kind of reference electrode used for fuel cells. It uses the potential of the hydrogen evolution reaction (HER) [22], and although the potential of the DHE contains a slight overvoltage caused by the reaction, it is hardly influenced by the environment such as some organic impurities. Therefore, it has been used for DMFC studies [23–27]. However, construction of the DHE is complicated due to geometric restriction and high contact resistance. For PEMFCs, a reversible hydrogen electrode (RHE) is generally used as the reference electrode [28,29]. Pure hydrogen gas is usually supplied to a separated channel for a reference electrode to avoid possible poisoning by impurity when a reformate is used as a fuel. Recently, several groups have evaluated the DMFC cathode with RHE configuration [30,31].

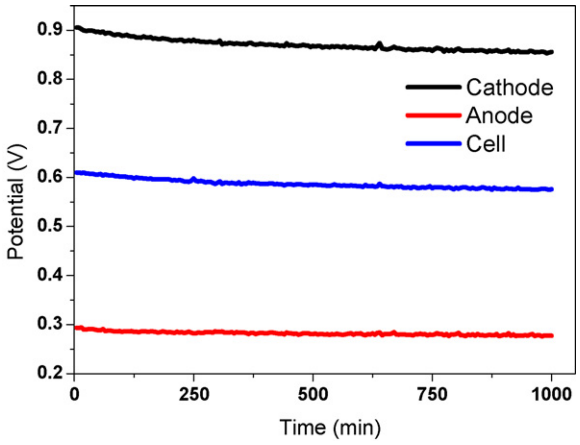

Fig. 1. Potential variation of individual electrode with function of time at OCV conditions. Cell temperature is 60 °C and 0.5 M methanol and air into anode and cathode, respectively.

In this study, we have performed a detailed analysis of direct liquid fuel cells by electrochemical impedance spectroscopy along with reversible hydrogen electrode under fuel cell operating conditions. We focused on formic acid rather than methanol since it has very different physical property as well as concentration dependence in fuel cell operation compared to DMFC. Additionally, two different kinds of anode diffusion media (DM) were evaluated to investigate the mass transfer characteristics of two different fuels.

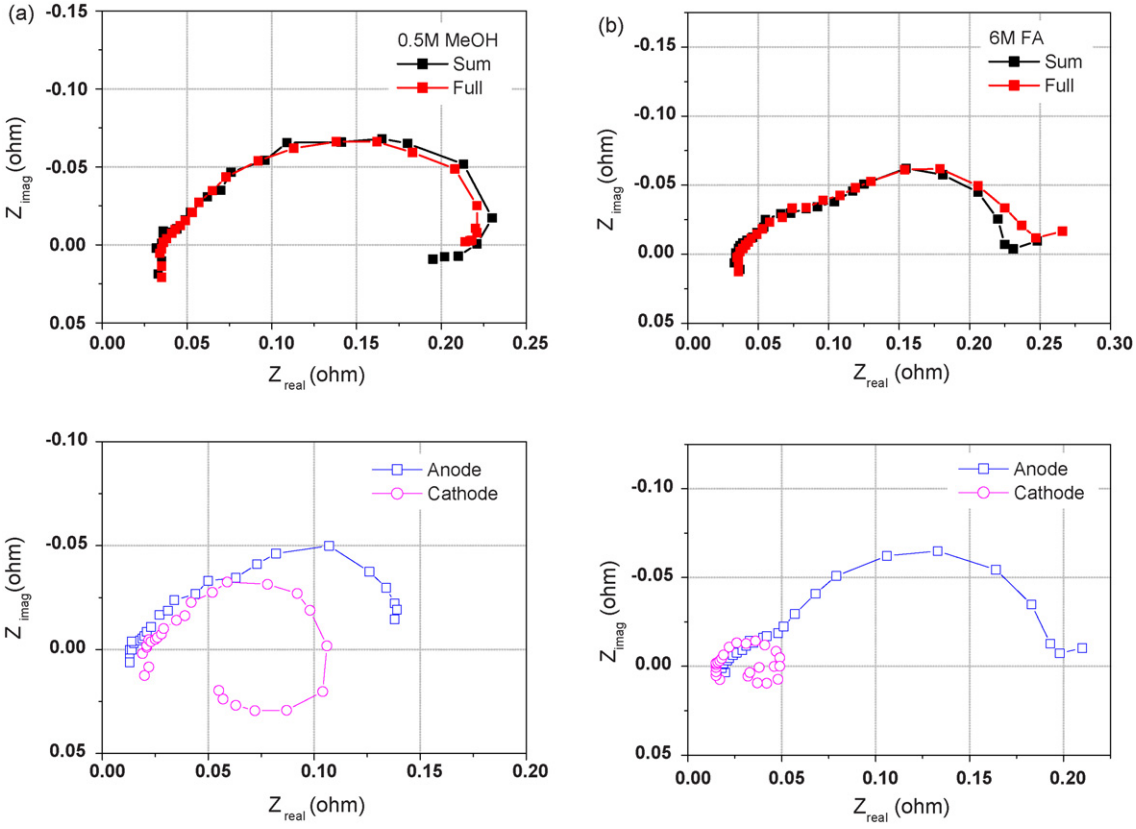

Fig. 2. Nyquist plots for a direct liquid fuel cell with (a) 0.5 M methanol and (b) 6 M formic acid at a current density of 100 mA cm^{-2}. Cell temperature is 60 °C, cathode air flow is 200 sccm, and liquid fuel flow is 5 ml min^{-2}, respectively.

2. Experimental

For a direct liquid fuel cell anode evaluation, two types of diffusion media were used; SGL 35AA (plain carbon paper) and SGL 25BC (microporous layer (MPL) coated hydrophobized carbon paper with 5% PTFE). On the cathode side, SGL 25BC was applied for membrane electrode assembly (MEA) testing. All carbon papers were used as received.

The membrane electrode assemblies were prepared as follows: the anode was Pt–Ru black (Johnson Matthey, 3.0 mg cm^{-2}) mixed with 10 wt.% Nafion solution. The cathode was constructed in a similar way to that of the anode with Pt black (Johnson Matthey, 3.0 mg cm^{-2}). The electrodes were placed on either side of a pretreated Nafion 115 membrane. The assembly was hot-pressed at 100 kg_f cm^{-2} for 5 min at 140 °C. The resulting MEA, with an electrode area of 10 cm^2, was sandwiched between two graphite blocks having serpentine flow path channels. In addition to the usual fuel cell hardware, reversible hydrogen electrode was installed as a reference electrode to resolve the anode and cathode performance. The RHE consists of Pt black coated gas diffusion electrode and Pt wire to which humidified hydrogen was supplied at 10 ml min^{-2} and 0.1 MPa. The Pt black coated gas diffusion electrode is used to minimize the overvoltage of reference electrode and contact resistance with membrane. The RHE is placed on the cathode side of an outer section of the Nafion membrane and the centre of the RHE is separated from the active area of membrane electrode assembly by 1 cm. It cannot only avoid contact with possible methanol or formic acid leakage but also minimize the instability by the changes in the water activity in the vicinity of the reference electrode caused by the electro-osmotic drag of water at a high current density. Also, special care should be taken to avoid misalignment of anode and cathode leading to uncertainty of potential measurement [32,33].

In order to evaluate the stability of the RHE reference electrode during operation of the fuel cell, its potential was periodically measured with respect to the open circuit potential of the fuel cell anode, which acts as an another reversible hydrogen electrode. The hydrogen fuel cell was operated with humidified H_2 on the anode and air on the cathode. The potential of the reference electrode was recorded at open circuit potential as well as during polarization measurements over the entire range of current densities. Only slight drift (within ±5 mV) of the potential of the reference electrode was observed over entire current densities, demonstrating the good stability of the reference electrode during fuel cell operation. The slight differences are likely to be mainly due to variations in the operation of the fuel cell with different MEA having small electrode misalignment. The stability of RHE can be validated once more by long-term stability in Fig. 1. During the normal DMFC open circuit conditions for 1000 min, any leakage of methanol and following potential deviation due to mixed potential was not observed except for only slight decrease of cathode potential caused by increase of methanol crossover rate with time.

The cell temperature was maintained at 60 °C and liquid fuel (formic acid and methanol) and humidified air (80% RH) were

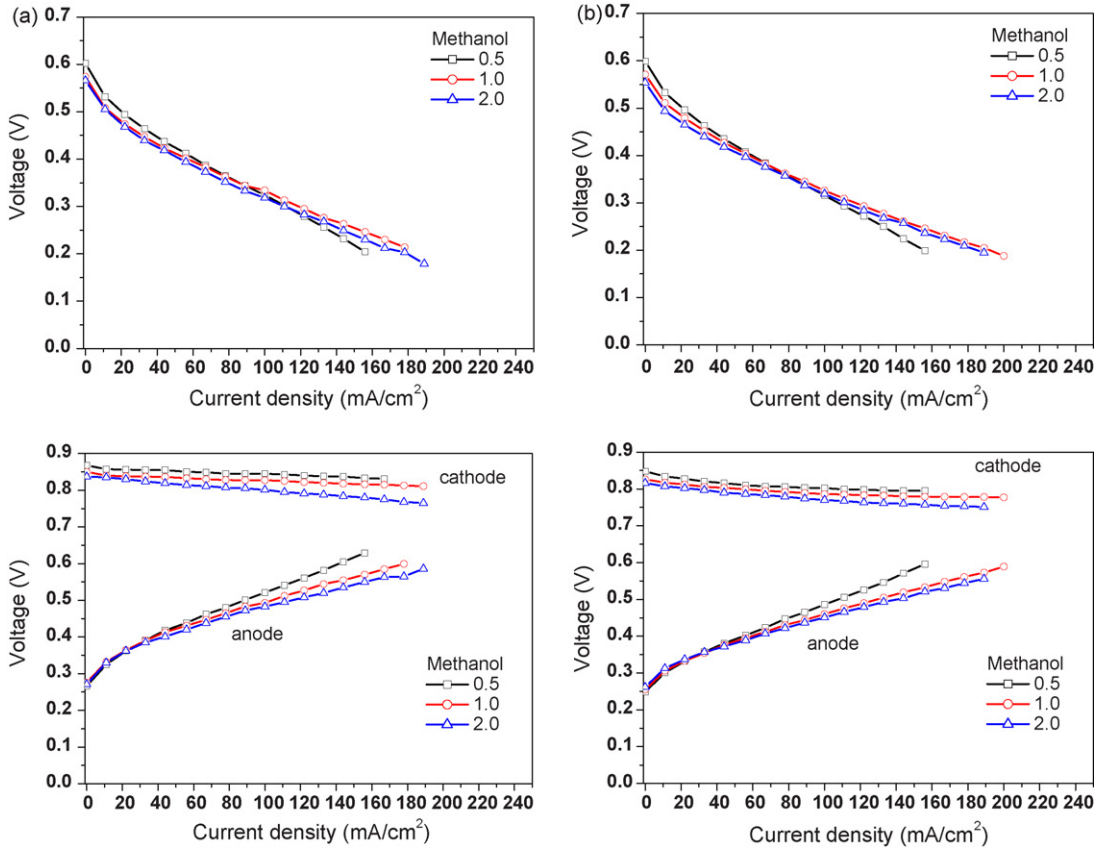

Fig. 3. Polarization curves and individual potentials of DMFC with different anode diffusion media. (a) Type A MEA and (b) type B MEA. Conditions as in Fig. 2.

applied at flow rates of 5 cc min^{-2} and 200 sccm, respectively. Conditioning was performed with 0.5 M methanol and 200 sccm humidified oxygen at ambient pressure. Current–potential transients were measured using an electronic load. Impedance spectra were measured using an Autolab PGSTAT30 (Eco Chemie) potentiostat/galvanostat with a frequency response analyzer (FRA). The frequency range investigated ranged from 10 kHz to 100 mHz with 10 points per decade. The amplitude of the sinusoidal current was adjusted to 10% of the steady current or lower.

3. Results and discussion

3.1. Stability of reversible hydrogen electrode

Fig. 2 shows nyquist plots for a direct liquid fuel cell (a) with 0.5 M methanol and (b) with 6 M formic acid at a current density of 100 mA cm^{-2}. Actually, the requirements of reference electrode for impedance are less stringent than for polarization measurements, since the anode and cathode impedances can be separated as long as the potential of the reference potential is not perturbed by the ac perturbation. As shown in Fig. 2, the sum of the individual anode and cathode impedances is in good agreement with full-cell impedance, providing good evidence that the separation of the impedance into anodic and cathodic components is reasonable and accurate except for slight deviation at low frequency region. Another noticeable feature of the impedance is that the high frequency resistance as well as individual charge transfer resistance can be separated. Generally, it can be expected that the cathodic high frequency resistance is higher than anodic one due to the better hydration of the membrane on the anode side by liquid fuel as shown in Fig. 2(a). However, this becomes more complicated if the membrane is not

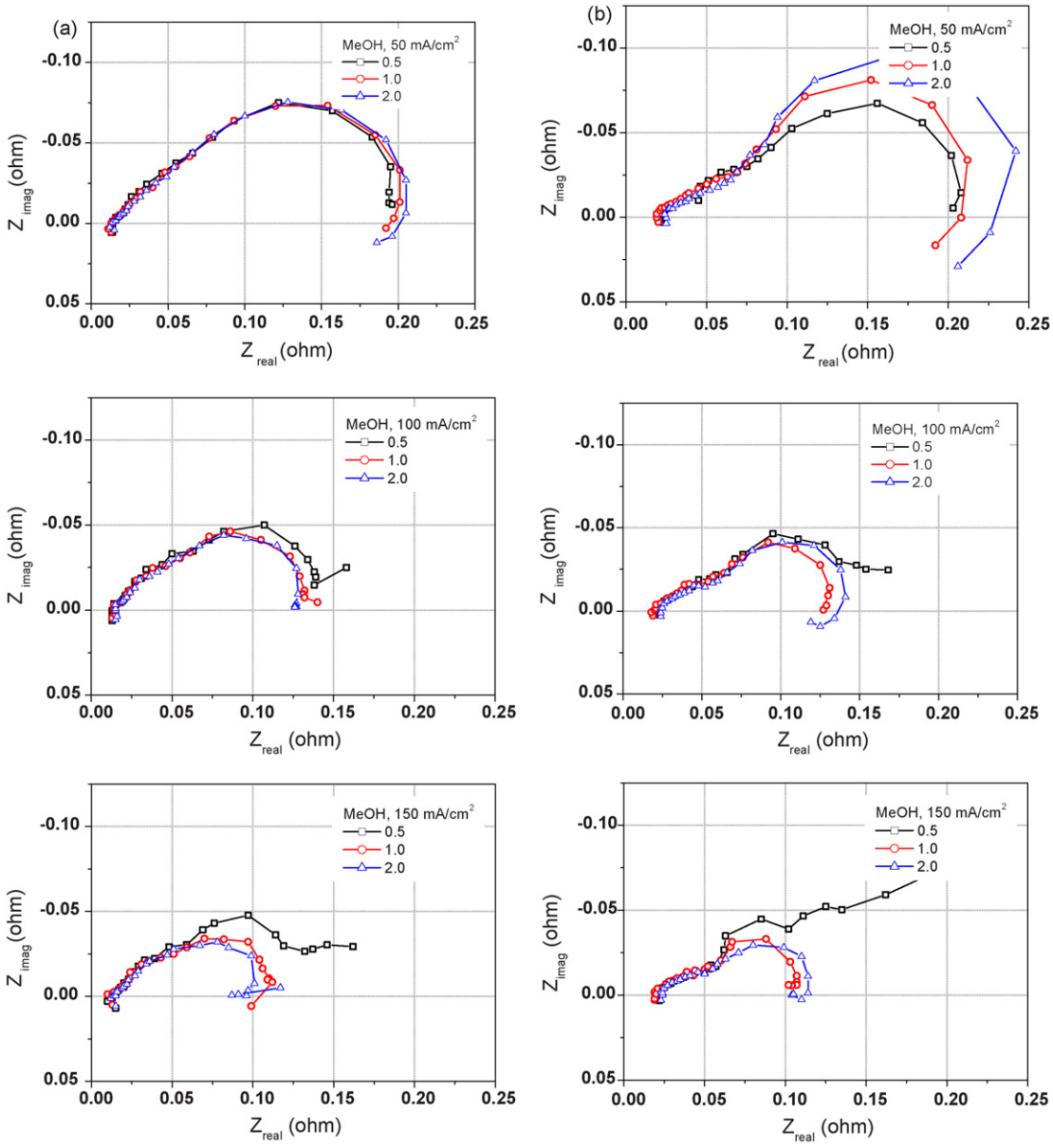

Fig. 4. Nyquist plots for a direct methanol fuel cell anode with an increase of current density and methanol concentration. (a) Type A and (b) type B. Conditions as in Fig. 2.

uniformly hydrated or anode catalyst layer has contact problems intrinsically which may be attributed to electrical conduction via an electrical double layer between the catalyst particle and electrolyte in the catalyst layer or to electronic conduction via grain boundaries between the electronic supply and the diffusion media. In case of the latter, not only the high frequency resistance increases slightly but also the high frequency capacitive loop can be obtained in the anode impedance, which remains constant with potential [34,35]. As a consequence, the anodic high frequency resistance becomes bigger than cathodic one despite of better hydration as shown in Fig. 2(b). In this study, we excluded the analysis of high frequency resistance with different MEA and anode diffusion media except for concentration dependence of formic acid.

3.2. Direct methanol fuel cells

The performance of direct liquid fuel cells is highly dependent on the property of individual component such as diffusion media or polymer electrolyte, which can dominate the transport of reactant(s) or product(s).

Fig. 3 shows the polarization curves of direct methanol fuel cell with different anode diffusion media. Type A is simple plain carbon paper based MEA, type B is microporous layer coated hydrophobized carbon paper based MEA. As shown in Fig. 3, there is little difference of performance and individual potential variation between two different anode diffusion media. Only conventional features with an increase of methanol concentration were observed over entire current densities except that the

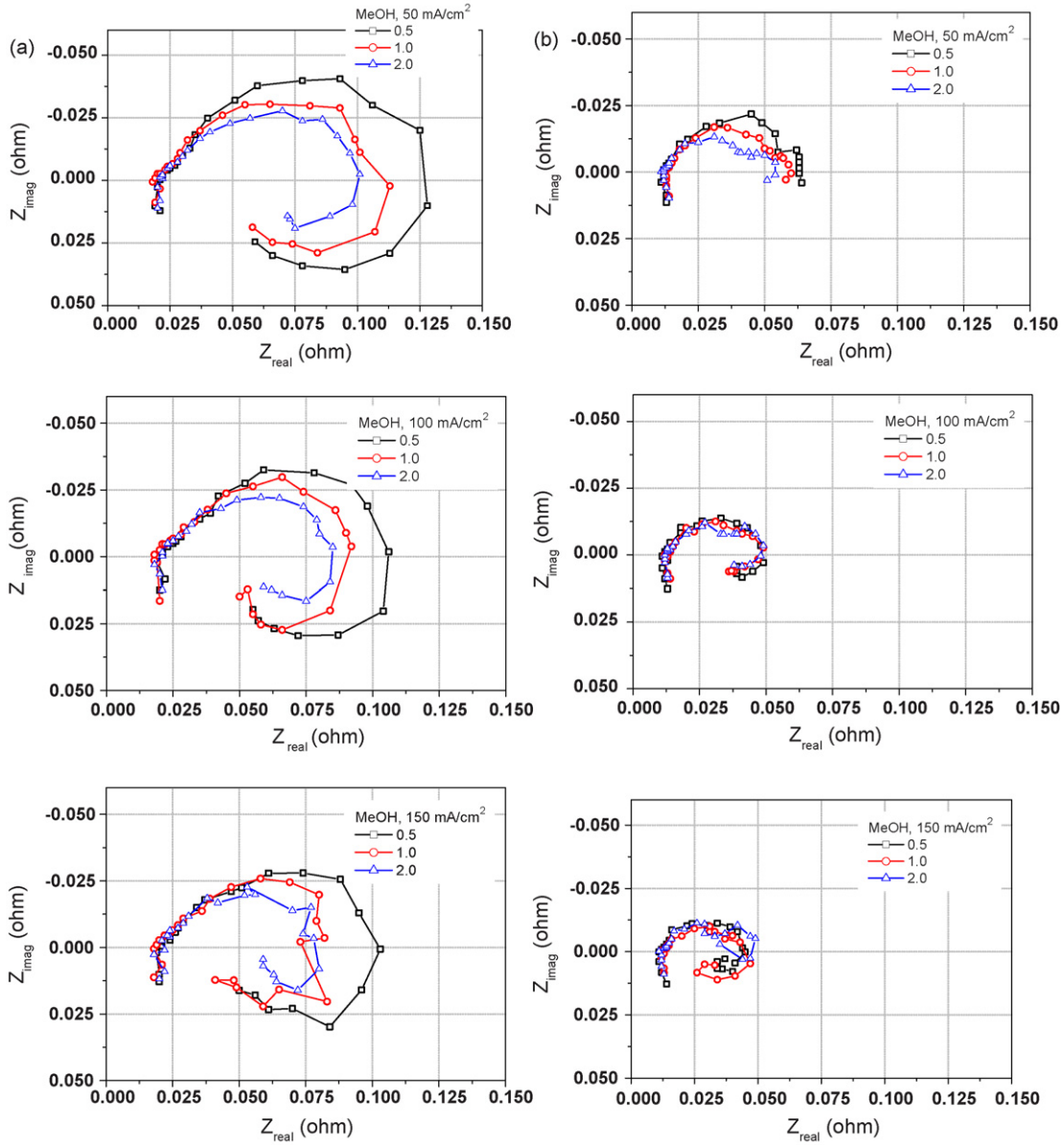

Fig. 5. Nyquist plots for a direct methanol fuel cell cathode with an increase of current density and methanol concentration. (a) Type A and (b) type B. Conditions as in Fig. 2.

individual potential of anode and cathode is a little bit different depending on the accessibility and crossover rate of methanol.

These results were supported by impedance spectra of individual electrodes. As shown in Fig. 4, the diameter of the capacitive circle in the anode spectra slightly increased with an increase of methanol concentration at low current density of 50 mA cm^{-2} on both anode diffusion media. The associated increase of charge transfer resistance with an increase of concentration pronounces a small auto-inhibitive effect in methanol oxidation. Contrary to literature for methanol oxidation on Pt [36], the order of methanol oxidation on Pt–Ru is fractionally negative at low current density. However, with an increase of current density, mass transfer limitation becomes dominant, resulting in Warburg behavior at low frequency region. Also, the charge transfer resistance on both anode diffusion media becomes almost same. The reason why the type B MEA induces a bigger auto-inhibitive behavior is not clear in this study, but it may be ascribed to the better accessibility of methanol to the catalyst surface through the more hydrophobic carbon paper, which may cause an increased charge transfer resistance due to increased poisoning by reaction intermediates. As a consequence, finding an optimal fuel concentration is very necessary to not only alleviate anode poisoning but also reduce fuel crossover, resulting in increasing the fuel efficiency.

Fig. 5 shows cathode impedance spectra recorded in a single cell with RHE at different current densities. Obviously, the type B MEA shows the smaller charge transfer resistance. It is largely due to the reduced crossover rate of methanol and water regardless of concentration or current density. However, such a big difference of impedance spectra was not reflected on the performance. Conversely, type A MEA has slight higher apparent cathode potential substantially. Another interesting thing is that charge transfer resistance decreased with an increase of methanol crossover rate and an inductive behavior is apparent in all cases similarly to the anode, which becomes less pronounced with an increase of current density. The plausible analysis will be done in the following section together with a direct formic acid fuel cell cathode.

3.3. Direct formic acid fuel cells

Fig. 6 shows the polarization curves of direct formic acid fuel cell with different anode diffusion media. Unlike methanol, formic acid suffers from significant mass transfer limitation with hydrophobic diffusion media due to its hygroscopic property. Thus, 1 M formic acid could not reach as much as current density of 50 mA cm^{-2} with type B MEA.

$$HCOOH \rightarrow CO_2 + 2H^+ + 2e^- \quad (1)$$

$$CH_3OH + H_2O \rightarrow CO_2 + 6H^+ + 6e^- \quad (2)$$

Actually, the electrochemical oxidation of formic acid (Reaction (1)) does not require water unlike methanol oxidation (Reaction (2)) according to its reaction mechanism although

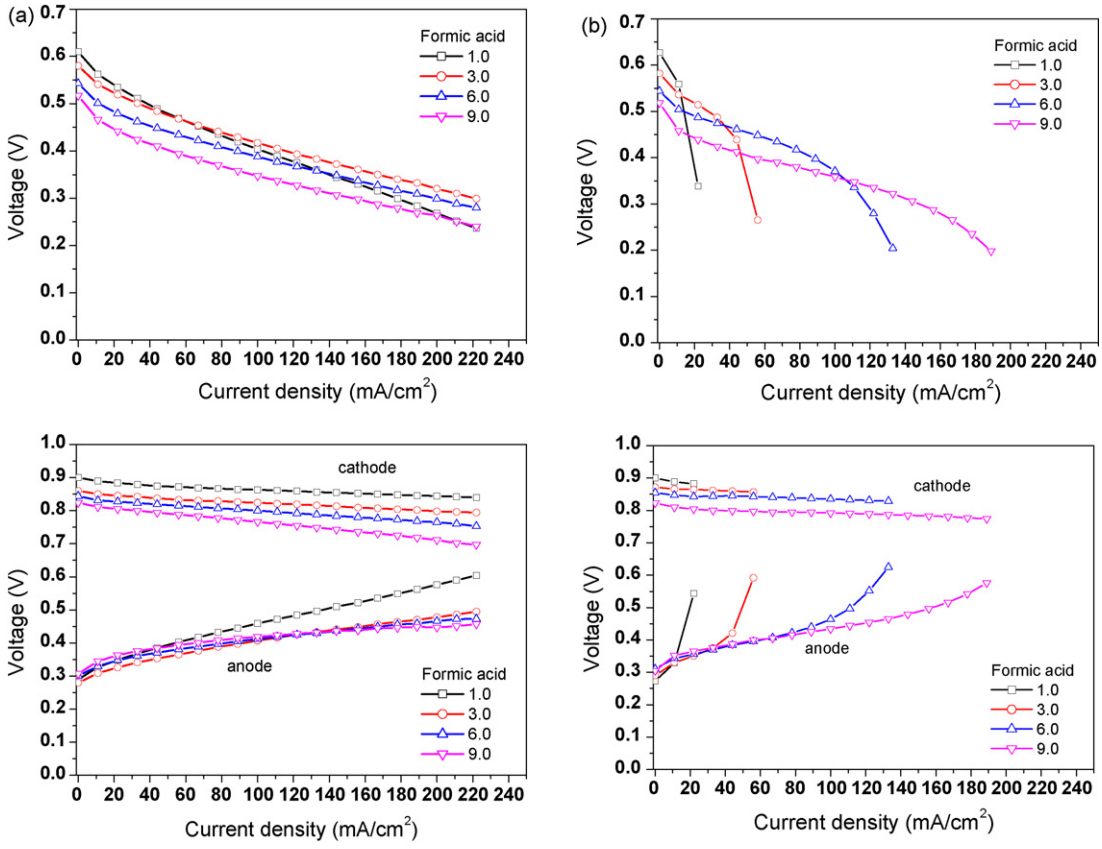

Fig. 6. Polarization curves and individual potentials of DFAFC with different anode diffusion media. (a) Type A and (b) type B. Conditions as in Fig. 2.

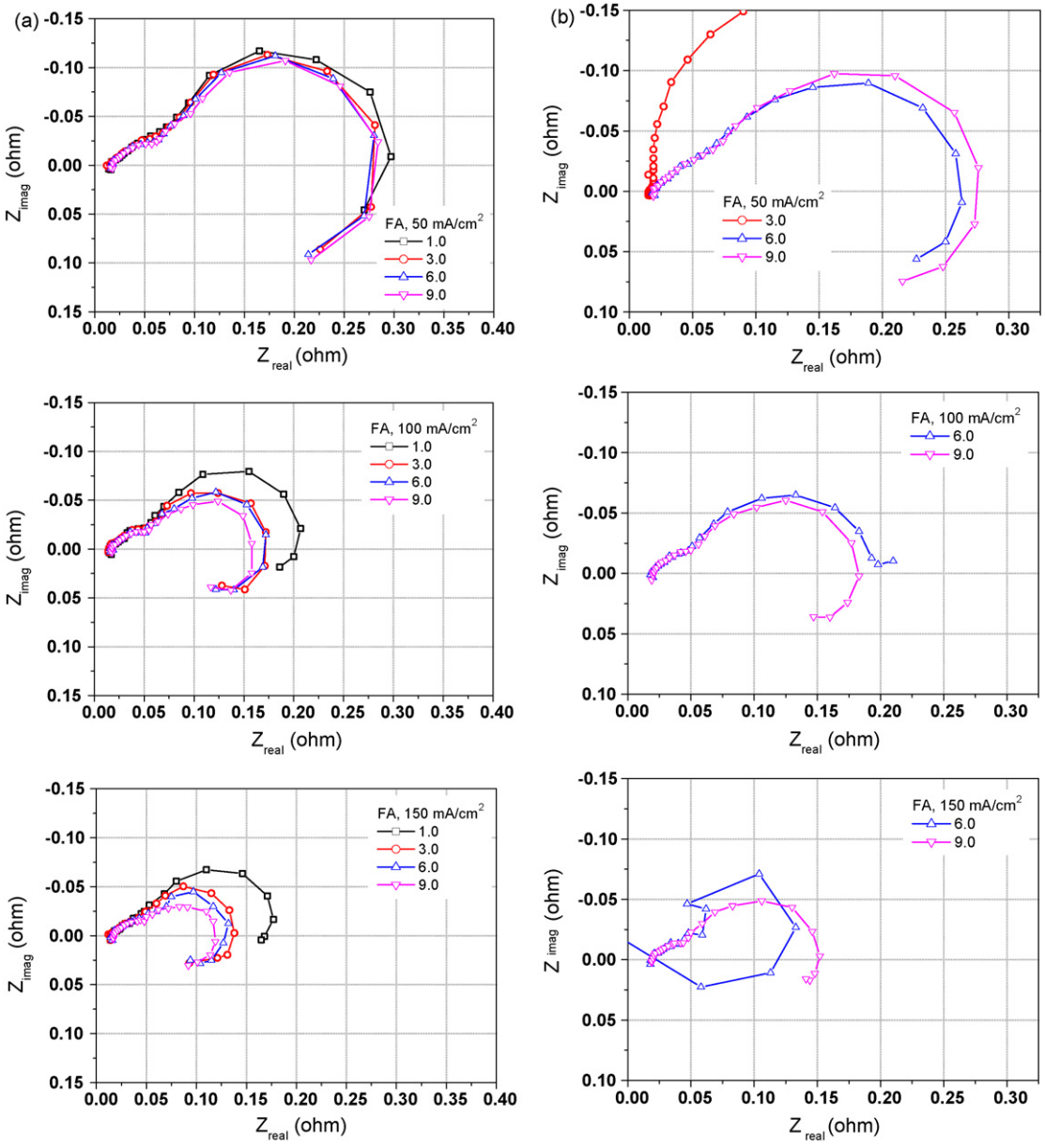

Fig. 7. Nyquist plots for a direct formic acid fuel cell anode with an increase of current density and formic acid concentration. (a) Type A and (b) type B. Conditions as in Fig. 2.

indirect path, which also requires water, is sometimes dominant depending on the catalyst. Therefore, plenty of water surrounding formic acid may be able to inhibit the electrochemical reaction on catalyst surface, thus the reaction may require more high concentration of formic acid near the catalyst surface compared to methanol. It can be identified by impedance spectra once more as shown in Figs. 7 and 8. In case of type B MEA (Fig. 7(b)), any data of 1 M formic acid cannot be obtained under galvanostatic mode. Even with a 6 M formic acid at higher current density, only very scattered, unusual results were observed at low frequency region. On the other hand, in case of type A MEA (Fig. 7(a)), similar trend was seen like methanol except that mass transfer limitation is dominant rather than auto-inhibitive behavior even at low current density.

Similarly to DMFC cathode, direct formic acid fuel cell cathode in type A MEA shows higher charge transfer resistance due to higher crossover rate. Another characteristic feature is that the high frequency resistance is highly dependent on the formic acid concentration. Even though such dependence is not clear in type B MEA whose crossover rate is not noticeable, type A MEA (Fig. 8(a)) shows very obvious concentration dependence. Namely, high frequency resistance increases with an increase of formic acid concentration. Fig. 9 shows the clear trends of concentration dependence of high frequency resistance in type A MEA in Fig. 8(a). The high frequency resistance increases linearly with respect to concentration of formic acid. This could be explained by hygroscopic property of formic acid and low content of water in the liquid fuel [37–39]. Highly concentrated formic acid fed in the anode may somewhat dehydrate cata-

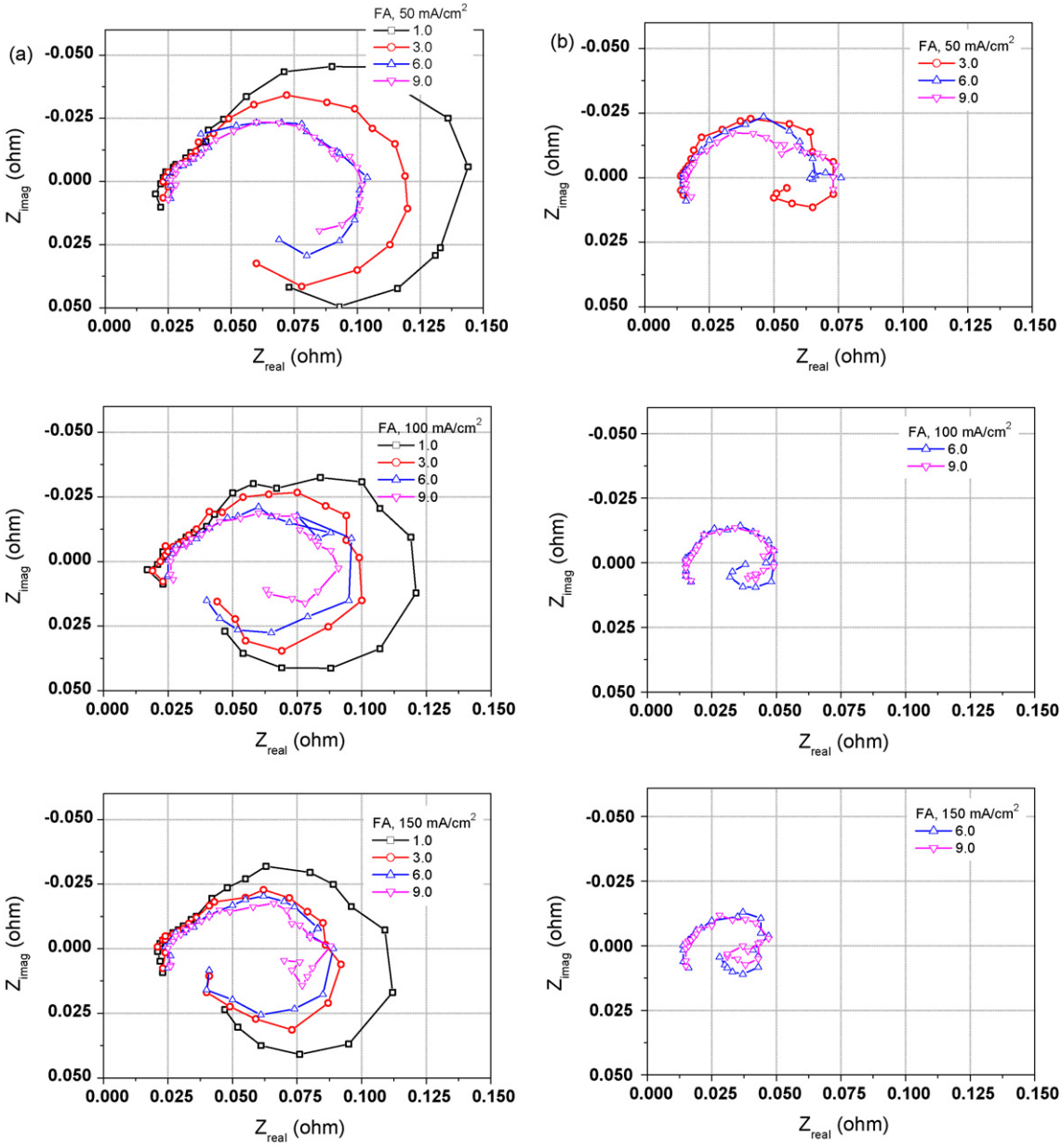

Fig. 8. Nyquist plots for a direct formic acid fuel cell cathode with an increase of current density and formic acid concentration. (a) Type A and (b) type B. Conditions as in Fig. 2.

lyst layer as well as membrane at mild temperature and hence reduce the formic acid and water crossover. However, such a dehydration effect does not significantly increase high frequency resistance in low concentration of formic acid. Thus, the high frequency resistance of the type B MEA was not influenced by dehydration effect due to its low crossover rate through membrane as well as anode catalyst layer. Based on the previous studies [40,41], membrane dehydration may increase the probability of degradation of membrane/cathode interface, resulting in questionable long-term durability. Therefore, the longevity of individual components as well as the system integration has to be taken into account at the same time, since more concentrated liquid fuel is more favorable to water management of system development.

As described in DMFC cathode section, direct liquid fuel cell cathode shows inductive behavior similarly to anode. Also, the charge transfer resistance decreases with an increase of crossover rate. Both behaviors become less pronounced with an increase of current density. To investigate a possibility that oxygen reduction reaction (ORR) is responsible for the inductive behavior for the cathode, inert impedance spectra with H_2O on the anode side were recorded using the same hardware and under the same operating conditions. The spectra in Fig. 10(a) show no inductive behavior for the cathode in the absence of any fuel fed in the anode. Also note that as the current density increases, the cathode spectra obtained in the presence of formic acid on the anode side (Fig. 10(b)) become very similar in shape and magnitude to those recorded with H_2O on

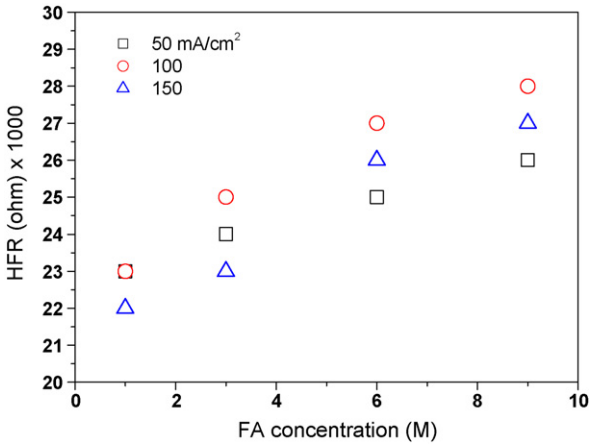

Fig. 9. High frequency resistance variation with respect to formic acid concentration extracted from Fig. 8(a).

the anode side. This is in good agreement with the fact that at high current density, most of the formic acid is oxidized at the anode catalyst layer and only a small amount penetrates to cathode.

Inductive behavior of the cathode is an indication that the local potential of the electrode is much lower than the average cathode potential ranging from 0.8 to 0.9 V. For this analysis, simple expression can be derived by assuming that the active site of the cathode can be divided into two separate parts, one

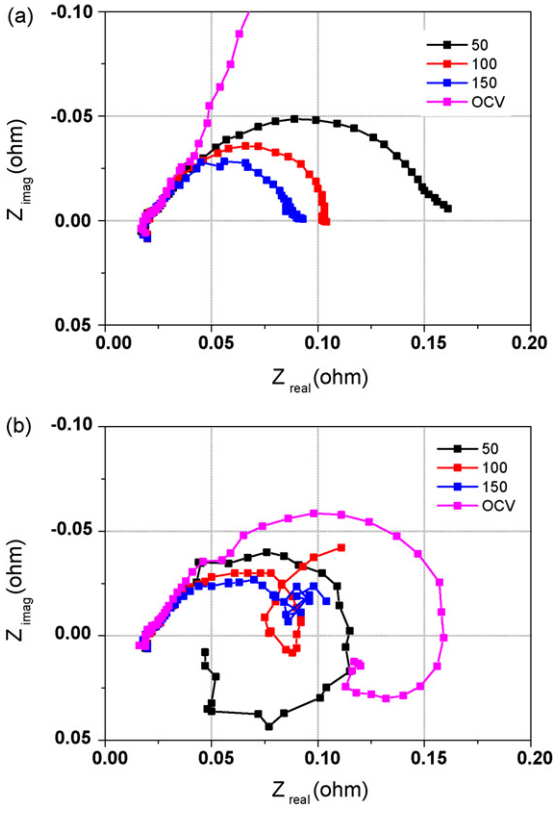

Fig. 10. Nyquist plots of the DLFC cathode at different current densities. (a) H_2O–air mode, (b) DFAFC mode with type A MEA, and 3 M formic acid. Conditions as in Fig. 2.

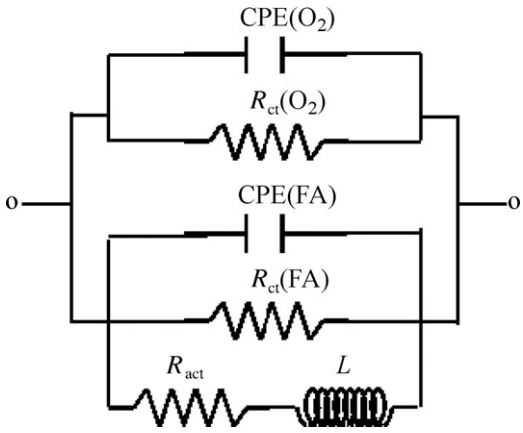

Fig. 11. Equivalent circuit for the impedance of DLFC cathode. R_{ct} and CPE are charge transfer resistance and constant phase element of oxygen reduction reaction and formic acid oxidation, respectively. R_{ad} is charge transfer resistance of reaction intermediate. L is inductance.

for oxygen reduction reaction and the other for oxidation of crossover formic acid [19]. The potential of the latter part can be close to that of an anode rather than the cathode. The oxygen reduction reaction in parallel with formic acid oxidation reaction can be depicted with corresponding equivalent circuit in Fig. 11. Also, the mixed charge transfer resistance can be expressed as following:

$$R_{ct}(\text{mixed}) = \frac{1}{R_{ct}(O_2)^{-1} + R_{ct}(FA)^{-1}} \quad (3)$$

According to the above equation, in order for the ORR kinetics to dominate the R_{ct}(mixed) value, R_{ct}(FA) must be significantly larger than $R_{ct}(O_2)$. This indicates that the potential of the formic acid oxidation part of the cathode must be much lower than the average cathode potential, perhaps as low as that of the anode. Theoretically, R_{ct}(FA) can be significantly larger than $R_{ct}(O_2)$ at such low potentials. Also, in order for the mixed charge transfer resistance to decrease with an increase of crossover rate of formic acid, smaller one has to decrease and bigger one has to increase based on this equation. This can be also explained by the assumption that surface oxygen species such as Pt–OH can be reduced by crossover formic acid [26]. Thus, the freshly reduced surface can provide free active surface area for ORR, consequently, reduce charge transfer resistance for oxygen reduction reaction to some extend depending on the total active sites available. In this study, since the relatively high metal loading of 3 mg cm^{-2} was used for a cathode, such an inversely proportional trend of charge transfer resistance with respect to crossover rate seems to be much clearer.

4. Conclusions

Direct liquid fuel cells were investigated by electrochemical impedance spectroscopy combined with reversible hydrogen electrode under fuel cell operating conditions. This powerful diagnostic tool can provide more comprehensive information of individual contribution to cell performance or transfer phenomena. In other words, the combination of an EIS with a

RHE cannot only single out individual polarization contributions but also separate the anode and cathode contributions at the same time. Unlike DMFCs, DFAFCs suffer from significant mass transfer limitations depending on the anode diffusion media property and formic acid concentration. Furthermore, the high frequency resistance of DFAFC cathode increases with an increase of formic acid concentration by dehydration effect due to its hygroscopic property. On both the DMFC and DFAFC cathodes, decrease in the charge transfer resistance with an increase of fuel crossover was observed together with a drop in the cathode potential. Based on the experimental observation, optimal selection of materials and operating conditions is necessary in view of fuel efficiency and long-term durability.

Acknowledgements

This work was supported by the Korea Science and Engineering Foundation(KOSEF) grant funded by the Korea government(MOST) (R01-2007-000-20290-0).

References

[1] S. Wasmus, A. Kuver, J. Electroanal. Chem. 461 (1999) 14.
[2] R. Chetty, K. Scott, Electrochim. Acta 52 (2007) 4073.
[3] A. Oedegaard, C. Hentschel, J. Power Sources 158 (2006) 177.
[4] S. Uhm, S.T. Chung, J. Lee, Electrochem. Commun. 9 (2007) 2027.
[5] S.J. Kang, J. Lee, J.K. Lee, C.Y. Chung, Y. Tak, J. Phys. Chem. B 110 (2006) 7270.
[6] R. Dillon, S. Srinivasan, A.S. Arico, V. Antonucci, J. Power Sources 127 (2004) 112.
[7] A.S. Arico, S. Srinivasan, V. Antonucci, Fuel Cells 1 (2001) 133.
[8] V. Gogel, T. Frey, Z. Yongsheng, K.A. Friedrich, L. Jorissen, J. Garche, J. Power Sources 127 (2004) 172.
[9] M. Neergat, T. Seiler, E.R. Savinova, U. Stimming, J. Electrochem. Soc. 153 (2006) A997.
[10] C. Rice, S. Ha, R.I. Masel, A. Wieckowski, J. Power Sources 115 (2003) 229.
[11] S. Ha, R. Larsen, R.I. Masel, J. Power Sources 144 (2005) 28.
[12] S. Ha, R. Larsen, Y. Zhu, R.I. Masel, Fuel Cells 4 (2005) 337.
[13] I.-M. Hsing, X. Wang, Y.-J. Leng, J. Electrochem. Soc. 149 (2002) A615.
[14] R. Jiang, H.R. Kunz, J.M. Fenton, J. Electrochem. Soc. 152 (2005) A1329.
[15] J.T. Muller, P.M. Urban, J. Power Sources 75 (1998) 139.
[16] J.T. Muller, P.M. Urban, W.F. Holderich, J. Power Sources 84 (1999) 157.
[17] J.-P. Diard, N. Glandut, P. Landaud, B.L. Gorrec, C. Montella, Electrochim. Acta 48 (2003) 555.
[18] D. Chakraborty, I. Chorkendorff, T. Hohannessen, J. Power Sources 162 (2006) 1010.
[19] P. Piela, R. Fields, P. Zelenay, J. Electrochem. Soc. 153 (2006) A1902.
[20] A. Oedegaard, J. Power Sources 157 (2006) 244.
[21] H. Kim, S.-J. Shin, Y.-g. Park, J. Song, H.-t. Kim, J. Power Sources 160 (2006) 440.
[22] J. Giner, J. Electrochem. Soc. 111 (1964) 376.
[23] A. Kuver, I. Vogel, W. Vielstich, J. Power Sources 52 (1994) 77.
[24] X. Ren, T.E. Springer, S. Gottesfeld, J. Electrochem. Soc. 147 (2000) 92.
[25] G. Li, P.G. Pickup, Electrochim. Acta 49 (2004) 4119.
[26] V.A. Paganin, E. Sitta, T. Iwasita, W. Vielstich, J. Appl. Electrochem. 35 (2005) 1239.
[27] Z. Siroma, R. Kakitsubo, N. Fujiwara, T. Ioroi, S.-I. Yamazaki, K. Yasuda, J. Power Sources 156 (2006) 284.
[28] T.E. Springer, M.S. Wilson, S. Gottesfeld, J. Electrochem. Soc. 140 (1993) 3513.
[29] S. Enback, G. Lindbergh, J. Electrochem. Soc. 152 (2005) A23.
[30] K. Furukawa, K. Okajima, M. Sudoh, J. Power Sources 139 (2005) 9.
[31] Y. Kim, W. Hong, S. Woo, H. Lee, J. Power Sources 159 (2006) 491.
[32] S.B. Adler, B.T. Henderson, M.A. Wilson, D.M. Taylor, R.E. Richards, Solid State Ionics 134 (2000) 35.
[33] W. He, T.V. Nguyen, J. Electrochem. Soc. 151 (2004) A185.
[34] O. Antoine, Y. Bultel, R. Durand, J. Electroanal. Chem. 499 (2001) 85.
[35] J. Otomo, X. Li, T. Kobayashi, C. Wen, H. Nagamoto, H. Takahashi, J. Electroanal. Chem. 573 (2004) 99.
[36] V.S. Bagotzky, Y.B. Vassiliev, Electrochim. Acta 12 (1967) 1323.
[37] I.V. Sukhno, V.Y. Buzko, V.T. Panyushkin, T.E. Dzhioev, I.A. Kovaleva, J. Struct. Chem. 44 (2003) 686.
[38] S. Aloisio, P.E. Hintze, V. Vaida, J. Phys. Chem. A 106 (2002) 363.
[39] Y. Zhu, S. Ha, R.I. Masel, J. Power Sources 130 (2004) 8.
[40] E. Endoh, S. Terazono, H. Widjaja, Y. Takimoto, Electrochem. Solid-State Lett. 7 (2004) A209.
[41] A. Collier, H. Wang, X.Z. Yuan, J. Zhang, D.P. Wilkinson, Int. J. Hydrogen Energy 31 (2006) 1838.